Large Area and Flexible Micro-Porous Piezoelectric Materials for Soft Robotic Skin

H. Khanbareh[1,2,3], K. de Boom[2], B. Schelen[4], R.B.N. Scharff[5], C.C.L. Wang[5], S. van der Zwaag[2], and P. Groen[2,6]

[1]*Materials and Structures Research Center (MAST), Department of Mechanical Engineering, University of Bath, Claverton Down, Bath, United Kingdom*

[2]*Novel Aerospace Materials Group, Faculty of Aerospace Engineering, Delft University of Technology, Kluyverweg 1, Delft, The Netherlands*

[3]*Materials Innovation Institute (M2i), Elektronicaweg 25, Delft, The Netherlands*

[4]*DEMO, Cooperate services, EWI, Delft University of Technology, Mekelweg 4, Delft, The Netherlands*

[5]*Soft Robotics Group, Faculty of Industrial Design, Delft University of Technology, Landbergstraat 15, Delft, The Netherlands*

[6]*Holst Center, TNO, High Tech Campus 31, Eindoven, The Netherlands*

August 23, 2017

Abstract

The need for flexible, highly sensitive tactile sensors that can fit onto curved surfaces is driving the conformable sensor materials research in the field of Human-Machine Interactions. Here we report a new type of compliant piezoelectric active composite, a micro-porous polyurethane-PZT material, capable of generating a voltage output upon touch. The composites are synthesized with the aim of maximizing the piezoelectric sensitivity of particulate composite sensor materials. The goal is to reduce the dielectric constant of the polymer matrix and improve flexibility of conventional bulk piezo-composites, consisting of ceramic particles in a dense polymeric matrix, by adding a third (gaseous) phase to the system in the form of uniformly sized pores. The presence of the gaseous component in the polymer matrix in the form of well-distributed spherical inclusions effectively decreases the polymer dielectric permittivity, which increases the piezoelectric voltage sensitivity (g_{33}) of the composite sensors significantly. The unique combination of dielectrophoretic structuring of PZT particles and the addition of a gaseous phase to the polymer resin results in the highest performance of the particulate composite sensors reported in the literature so far. The newly developed micro-porous composites show g_{33} value of 165 mV.m/N that is twice that of the structured PZT-bulk PU composites (80 mV.m/N) and more than

five times the g_{33} value of bulk PZT ceramics (24-28 mV.m/N). The capability of the flexible freestanding sensors for application in touch sensing devices for soft robotics is demonstrated.

1 Introduction

The development of human-like skin with multi-sensory capabilities can revolutionize orthotics, prosthetics as well as autonomous intelligent robotics. These robots with enhanced human-machine functionalities can have extended range of applications in care and exploratory areas [1]. The most important function of skin is the sense of touch which includes normal static force, tensile strain, shear force as well as vibration sensing. Different transduction methods, based on resistive [2–6], capacitive [4, 7, 8], magneto resistive [9], optic [10, 11] and piezoelectric materials [3, 12–15], provide these different sensing capabilities. This primary function of the skin to perceive contact force can be integrated in sensor arrays. The need to mimic the mechanical properties of human skin, in particular the flexibility, to accommodate various motions is the second key function that should be taken into account. Thus the choice of materials is critical to achieve desired functional and mechanical properties. Here, we report a micro-porous piezoelectric active composite capable of generating a voltage output upon human touch. The composite was synthesized by mixing ferroelectric ceramic particles in a rubber polymer matrix, while gas was added to the system through a foaming process to enhance the piezoelectric voltage sensitivity by reducing the permittivity of the composite.

Porous dielectric polymers have been shown to achieve ultra low permittivity for the next generations of microchips. Such microchips require interlayer of dielectrics with dielectric constants below 2.2. The porous structures is often achieved by thermal decomposition of a block copolymer composed of a thermally stable block and a thermally unstable one [16]. These porous materials show a clear relation between decreasing permittivity and increasing porosity [17]. The macroscopic behavior of such porous polymers is determined by a combination of the intrinsic constitutive behavior of the polymeric material, and the microstructure. There are numerous models in literature that relate material properties of the porous polymers to the intrinsic properties of the constituent phases. A simple simulation based on the mixed connectivity model [18] in a serial and a parallel arrangement, can be used to estimate the dielectric properties of the porous polymer. A two-phase dielectric material, consisting of spherical gaseous inclusions in a polymer matrix, is assumed. In the serial mode (0-3), the porosities are homogeneously distributed in the polymer matrix. In the parallel mode (1-3), the microstructure can be considered as the columns of porosity, elongated in the thickness direction. With increasing the gaseous content, the dielectric constant of the porous polymer decreases linearly. However, in a system of homogeneously distributed air inclusions in the polymer matrix, the dielectric constant of the porous foam decreases exponentially with increasing gaseous content [19, 20]. Therefore, a porous polymer material consisting of randomly distributed closed cells, has an effectively reduced dielectric constant compared to the bulk polymer.

As far as piezoelectric properties of the ceramic-polymer composite sensors are concerned, optimization of the dielectric properties of the polymer matrix plays an important role in controlling the output voltage of the di-phase composites [21]. The piezoelectric voltage sensitivity, g_{33}, is calculated by dividing the d_{33} of the composites by their relative permittivity. Therefore, the piezoelectric performance of the di-phase systems can be enhanced by adding a gaseous phase to the polymer matrix, in form of a homogeneously distributed porosity (0-3 connectivity) to decrease the dielectric constant,

while d_{33} remains unchanged.

A further improvement in d_{33} can be obtained by structuring the ferroelectric particles in the polymer walls of the porous polymer via dielectrophoresis (DEP) as was shown for bulk polymer-PT composites [22, 23]. The behavior of a micro-porous piezoelectric composite materials is controlled by geometrical, topological, elastic, dielectric, and piezoelectric parameters [23]. In this paper, the influence of topological parameters on the properties of the porous polyurethane (PU) is mapped in detail. Micro-porous composites of PZT-micro-porous PU are manufactured and their functional properties are investigated. Details of the manufacturing procedure are discussed in the experimental section at the end of the paper.

2 Experimental procedure

2.1 Composite manufacturing

Lead zirconate titanate ceramic powder (PZT5A4), provided by Morgan Electro Ceramics, was calcined at 1150 °C 1 h in a closed zirconia crucible according to the optimized scheme reported by Van den Ende [24]. After calcination, the powder was dry ball milled for 2 h in a Gladstone-Engineering G90 jar mill. Subsequently, the particles were sieved for 20 min, using a Haver & Boecker EML Digital Plus test sieve shaker with stacked sieves with mesh sizes of 125 μm and 63 μm. The powder was dried for at least 2 h to prevent agglomerations due to moisture, as well as chemical interaction between the polymer and moisture from the particles. The particle size distribution of milled powder in an aqueous solution with 10% isopropyl alcohol, measured by a Beckman Coulter LS230 laser diffraction analyzer, was found to be $d(10) = 0.8$ μm, $d(50) = 1.8$ μm, and $d(90) = 6$ μm.

A two component urethane rubber, Smooth-on-Econ 80 Polyurethane, is used to serve as the polymer phase in the composites studied in this paper. This polymer is composed of di-isocyanate (component A) resin and polyol (component B) (see Fig. 1). Gas formation is observed upon addition of water to the uncured polymer, due to a chemical reaction between di-isocyanates and water, which leads to the formation of poly(urea-urethane), and the release of CO_2 (Fig. 1).

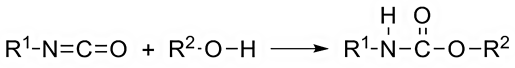

(a) Chemical reaction of di-isocyanates with polyols.

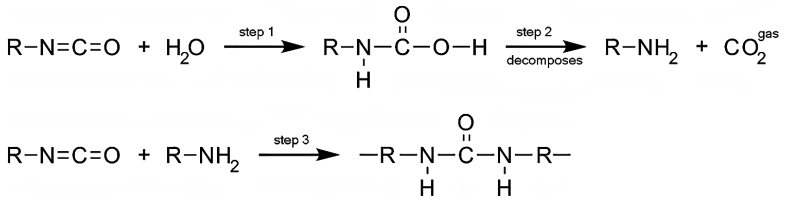

(b) Chemical reaction of di-isocyanates with water and the release of CO_2.

Figure 1: Chemical reaction of PU.

To study the effect of demineralised water (D-water) additions on gas formation in PU, component A was magnetically stirred at 600 RPM for 6-7 min at room temperature to create nucleation sites for the produced gas to flow into. In the meantime, component B and a varying amount of D-water , from 0 to 0.5%, was mixed using a Speedmixer DAC 150.1 FVZ at 3500 RPM for 5 min. Subsequently, component A, B and D-water were magnetically stirred at 600 RPM, until

the viscosity increase stopped the magnet stirring. A tape-cast-film was made on an Aluminum substrate, using a doctor blade that was set at 1 mm. The amount of D-water that was added to 10 mL PU is in the μL range. Influences from moisture in the air can thus be significant, which is why the samples were stored in a controlled environment and further processed on the same day.

Thermogravimetric Analysis (TGA) of the polymer is performed using Perkin Elmer Pyris Diamond at 20°C/min under a nitrogen atmosphere. The results show that, at 200°C, less than 2wt% loss is registered. Subsequently, Differential Scanning Calorimetry (DSC) was performed, at a heating rate of 20 °C/min under a nitrogen atmosphere, using the Perkin Elmer Sapphire to find the glass transition temperature, T_g, of -7.6 °C. The T_g of the polymer does not appear to be significantly affected by post curing at 100 °C.

The route, that was used for the production of the D-water range of 0 to 0.5%, as explained before, was also used for the production of the first batch of random (0-3) micro-porous composites. However, for the 20 vol% PZT, the initial viscosity of the system due to the presence of the PZT was too high to allow for magnetic stirring. The production route was adapted by elimination of the magnetic stirring step accordingly. Porous samples were able to form nonetheless. To check the necessity of the magnetic stirring in the D-water sample production, a PU cast was made where PU component A, component B and the D-water were mixed all at once for 60 seconds at 3500 RPM. The result was a cast with large (>1 mm) through-thickness voids and some smaller voids of approximately 100 μm, distributed throughout the cast. This rules out self-nucleation as a possible reason for the foaming of non-mechanically stirred PZT-porous PU samples, and proves that micro-voids are essential in order to obtain a desirable porous micro-structure. It also proves, that PZT particles are able to function as void nucleation sites, thereby replacing the functionality of micro-voids which are introduced by magnetic stirring.

To prepare the composites, the PZT particles were dispersed in the mixture of polymer resin and demineralized-water (D-water), as shown in Fig. 2-a, to the specific PZT volume fractions of 0%, 20%, 30% and 40% and mixed at 3500 RPM for 1 min. 0-3 samples were produced by casting the slurry on an Aluminum substrate using a doctor blade at the thickness of 1 mm. The surface of the film was exposed to air. DEP alignment of the PZT particles in the porous polymer was done in a closed mold format using a Teflon mold of 1 mm thick. The details of the mold layout are presented elsewhere [22]. For random and structured samples, the optimum volume fraction of D-water, resulting in maximum reduction of dielectric constant of the polymer matrix is found to be 0.4 vol% and 0.2 vol%, respectively. This optimization will be discussed in detail in the following section. The closed mold used in preparation of DEP structured samples restricts the water evaporation from the mixture, therefore, a lower water content of 0.2 vol% results in similar gas content of 60 vol% similarly as in random composites prepared by casting. The dielectrophoretic structuring (Fig. 2-b) is performed on uncured composites by applying an electric field of 3 kV/mm at 3 kHz for 1.5 h, using a function generator (Agilent, 33210A) coupled to a high voltage amplifier (Radiant Technologies Inc., T6000HVA-2), until the polymer matrix is fully cured. After curing, flexible films of 1 mm thickness were obtained. The samples were then poled for 2 h, using a Heinzinger 30000-5 30kV DC amplifier, a Haake N3 digital circulating hot oil bath filled with silicone oil and a custom made sample holder, as presented in Fig. 2-c, at 100 °C, 5 kV/mm.

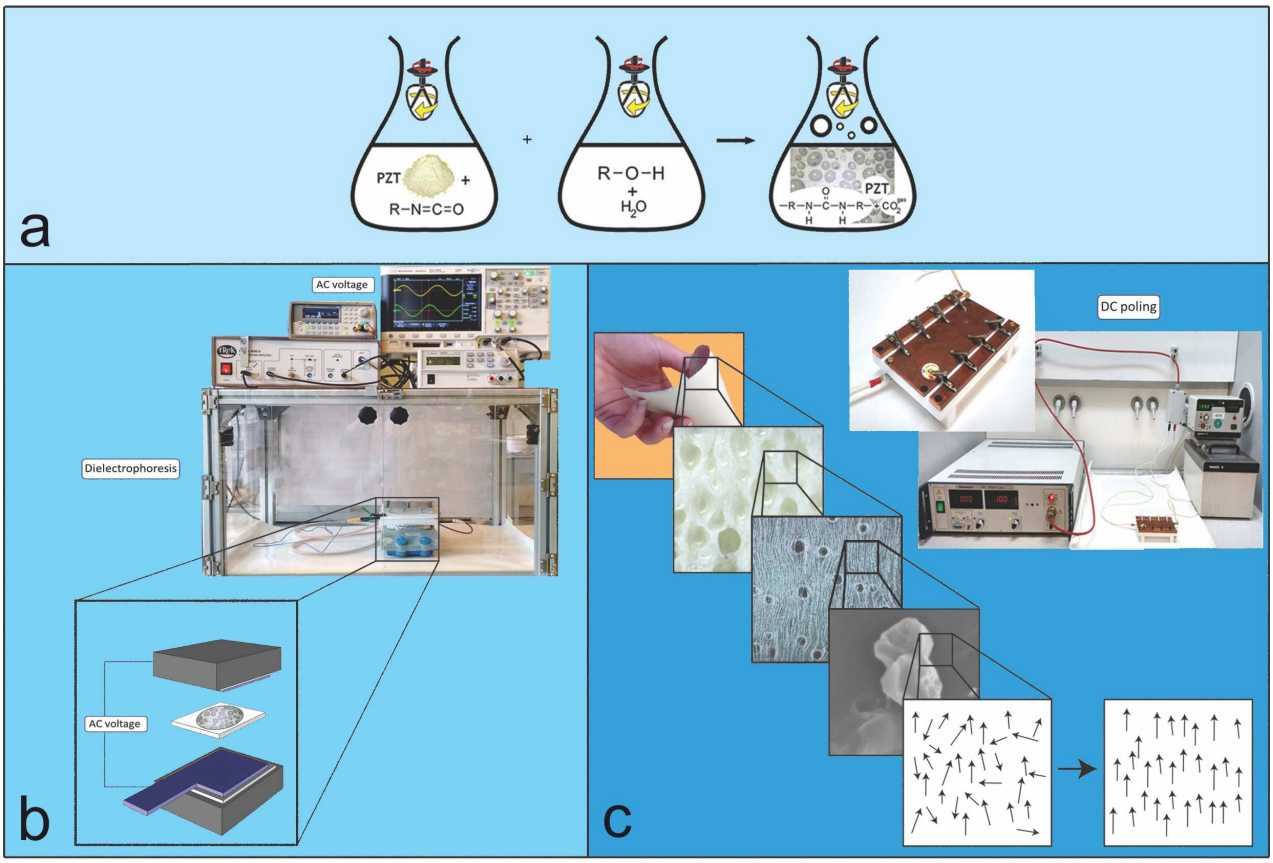

Figure 2: Manufacturing of the micro-micro-porous piezoelectric sensors. (a) Chemical reaction of the polymer with water and mixing PZT powder. (b) Dielectrophoresis process. (c) Microstructure evolution of the micro-porous sensors after DEP and poling.

2.2 Measurement procedure

Circular discs of 18 mm were produced, and electrodes were made by sputtering of Gold for 20 min on both sides using a Quorum Q300T D sputter coater. Subsequently, all samples were punched using a 16 mm punch, thereby removing the material at the edges to prevent leakage current. The dielectric constant of the composites was determined using an Agilent 4263B & 16034E - Inductance Capacitance Resistance Meter (LCR) by the parallel plate capacitor method at 1 V and 1 kHz. The d_{33} of the poled samples were determined using the Piezotest PiezoMeter System PM300 - Berlincourt d_{33} meter, under a 10 N static force and a 0.25 N dynamic force at a frequency of 110 Hz. At least three samples of each composite were tested. For microstructural analysis the samples were sectioned using scissors along the thickness and the cross sections were observed using a field emission-scanning electron microscope (FE-SEM) (JEOL, JSM-7500F). The tensile properties of the materials were tested using an Instron 3369 machine with a 50N load cell and a strain rate of 5 mm/min at room temperature. Rectangular specimens with dimensions 30 mm × 5 mm × 1 mm were used.

3 Results and discussion

3.1 Microstructures of porous PU-polymer and PZT-micro-porous PU composites

The polymer material used in this study is a commercial polyurethane (PU) composed of a di-isocyanate resin and a polyol. Gas formation is observed upon addition of water to the uncured polymer, due to a chemical reaction between the di-isocyanates component and water, which leads to the formation of poly(urea-urethane), and the release of CO_2. The effect of demineralised water (D-water) content, ranging from 0 to 0.5%, on the microstructures of PU is investigated. The microstructures are shown in Fig. 3. The increase of the gaseous volume fraction and sample thickness with increasing water content is clearly visible.

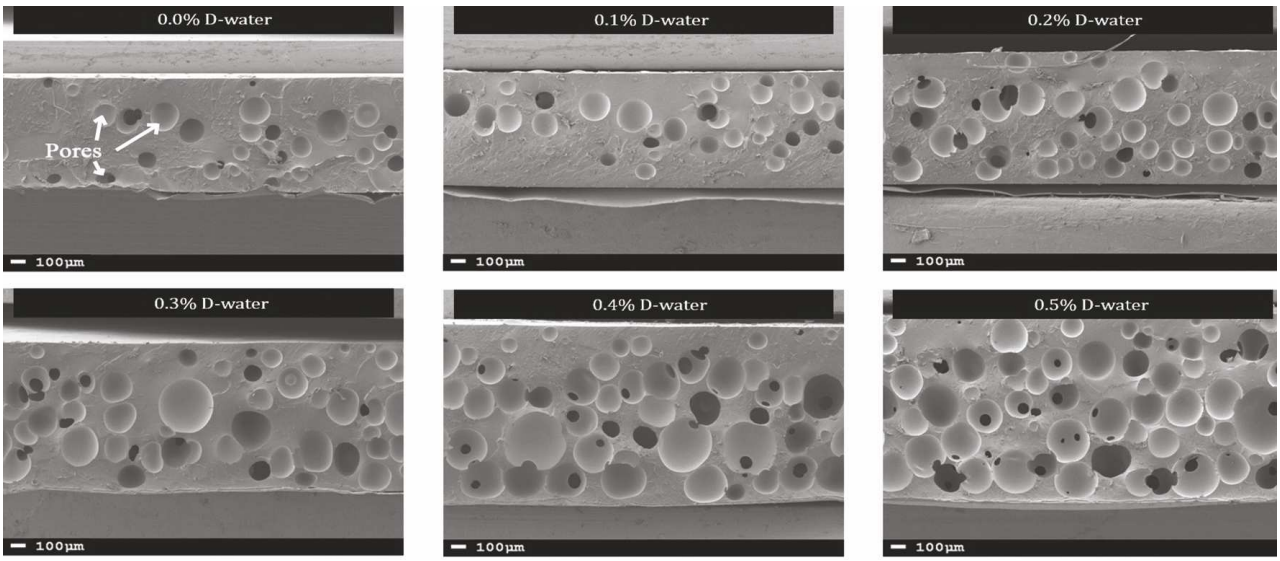

Figure 3: SEM microstructures of neat PU polymers containing different volume fractions of D-water, ranging from 0.0% to 0.5%.

The SEM images are processed using the Image Processing Toolbox of MATLAB, in order to quantify the gaseous volume fraction, pore size and morphology. The images are binarized, and the area fraction of the gaseous phase, as an indication of the volume fraction of this phase, is subsequently calculated. Increasing the D-water content results in increasing the gas production in the polymer, which is entrapped in a primarily closed cell porous structure. A linear correlation is observed between the gas content and the corresponding water content.

The pore size distribution, as a function of the water content, is shown in Fig. 4-a. The diameter is an equivalent circular diameter, calculated by conversion of individual pore areas to the diameter of a corresponding circular pore. The minimum diameter does not show significant changes with increasing the water content. However, the average and maximum diameters increase with rising the D-water content. The 0.5% D-water sample shows the highest average diameter of 260 μm.

The volume fraction of the open cells, observed on the micro-porous-PU microstructures, is calculated using the area fraction of the open cells with respect to the total area of the cells. The results at different D-water contents are shown in Fig. 4-b. Increasing the water content, thus increasing the gas volume fraction, leads to cell walls merging that results in a higher content of open cells.

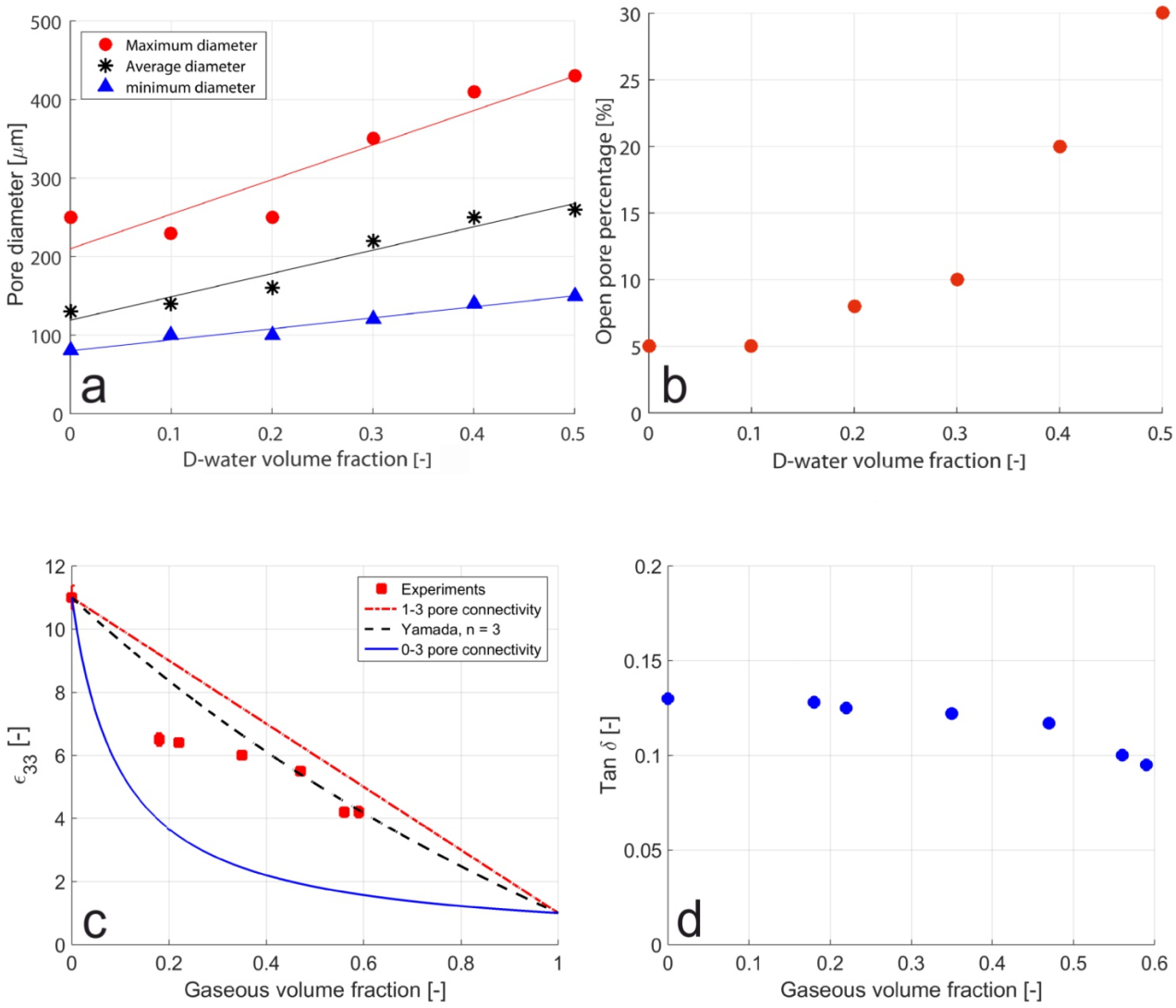

Figure 4: Variation of (a) pore size, (b) open pore content, (c) dielectric constant and (d) dielectric loss of neat porous PU as a function of D-water content.

The pore shape is characterized using the aspect ratio, AR, as a measure of elongation. AR approaches infinity for a long object, while an isotropic object has AR of 1. The pore AR at different D-water content ranges between 1 and 1.3 which is very close to that of perfect spheres.

The microstructures of random and dielectrophoretically (DEP) structured PZT-micro-porous PU composites are shown in Fig. 5 for a PZT volume content of 20%. Samples show a uniform distribution of pores and ceramic particles. Agglomerations are only observed at high volume contents of 40 vol% PZT. In DEP structured microstructures the pores are likely to be affected by the application of the AC electric field during DEP, thus showing elongation in the field direction. The PZT particle chain formation is present throughout the entire sample, but most clearly visible in the cell walls due to the smoothness of the surface. The same observations hold for the microstructures of the composites with PZT content of 10%, 30% and 40%.

Addition of 0.4% D-water in the random composites of PZT in PU has successfully resulted in roughly 60 vol% of gas in these samples. In structured composites of PZT in PU, prepared in a closed mold, addition of 0.2% D-water has resulted

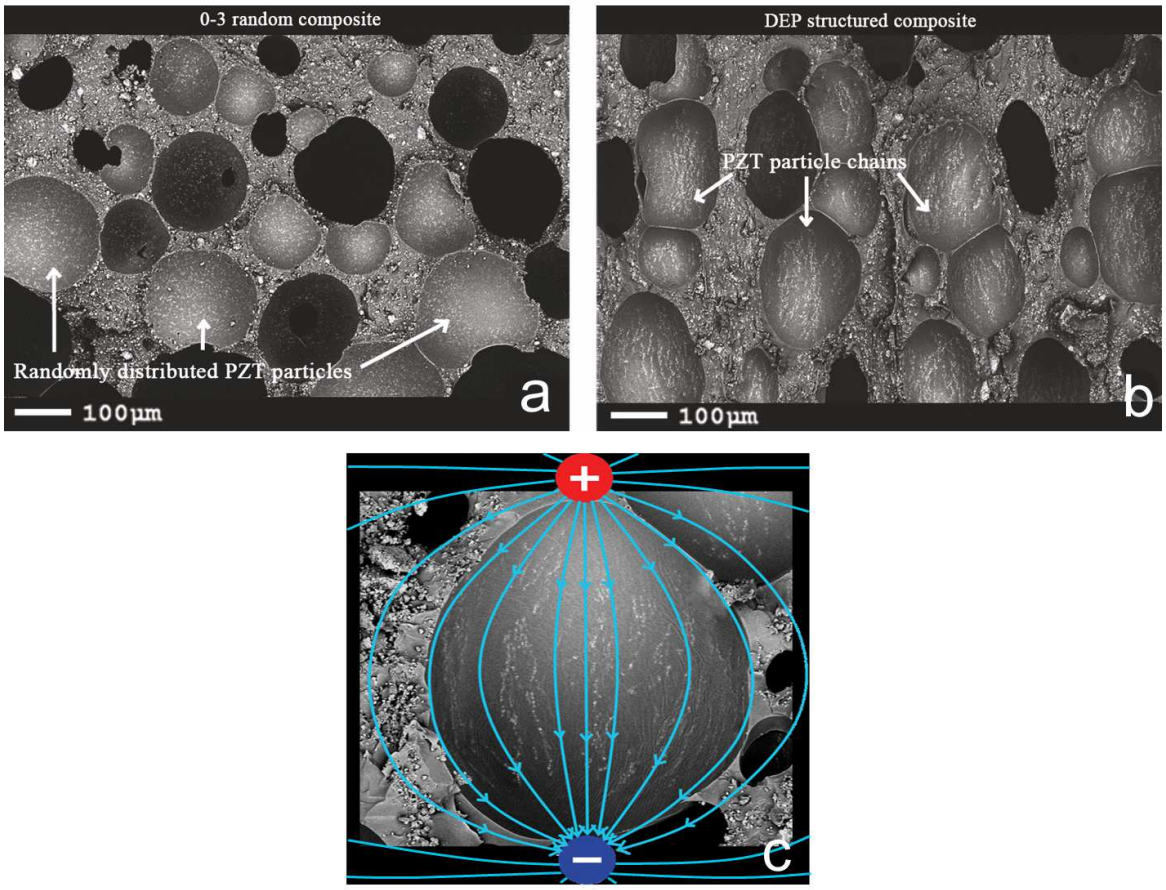

Figure 5: SEM microstructures of (a) of 0-3 and (b) DEP structured micro-porous composites of 20% PZT in PU prepared using 0.2 vol% D-water. (c) Chain formation along the electric field lines during dielectrophoresis.

in almost 60 vol% of gaseous phase.

The average pore diameters for random and structured PZT-micro-porous PU composites are calculated. The average pore size in structured composites varies from 250 μm to 100 μm with increasing the PZT content from 0% to 40%, respectively. Increasing the PZT volume fraction results in higher viscosity of the composites, which restricts the pore growth. The same trend is observed in random composites, containing PZT ranging from 20% to 40%. However, the random 10% PZT-micro-porous PU sample shows a large average pore diameter of 400 μm. The reason can be partially attributed to the low viscosity of this sample which accommodates the voids on the bottom of the film to merge until they form large pores, while the smaller voids closer to the top escape the film. Secondly it can be attributed to the the presence of less nucleation sites in the form of PZT particles in the composites of 10% PZT-micro-porous PU.

The aspect ratios of the pores in the random and structured PZT-micro-porous PU composites are calculated. The random composites of varying PZT content show consistent AR, close to 1, which indicates spherical voids as shown in Fig. 5. However, the DEP structured composites show elongated pores in the field direction. A maximum AR of 1.7 is observed for the structured 30% PZT-micro-porous PU composite.

The open pore content is calculated for different PZT content in random and structured composites. Increasing the PZT volume content from 0 to 40% results in a small increase of open pore content, in both random and structured composites. A maximum pore volume fraction of 0.3 is observed for the 40% PZT-micro-porous PU sample.

3.2 Properties of composites

The effect of gaseous volume fraction on the dielectric constant (ϵ_{33}) of the micro-porous PU-PZT composites at 1 kHz is shown in Fig. 4-c. The dielectric constant decreases noticeably with increasing porosity, as the increasing amount of air ultimately leads to a permittivity value of one. The presence of 56 vol% gas results in a 62% reduction in the dielectric constant from 11.1 to 4.2.

Considering the porous polymer a di-phase composite, consisting of a gaseous phase in a polymer matrix, the properties of the material can be simulated using Yamada's model [25]. The dielectric constant of the neat PU polymer is measured to be 11.1 at 1 kHz. To fit the experimental data to the model an n value of 3 is used, which corresponds to aspect ratios of 1, that is an indication of spherical gas inclusions. This is in agreement with the AR of the porosities calculated from the SEM microstructures, shown in Fig. 5. The lower and upper bounds of the dielectric constant can be simulated using serial and parallel arrangements, based on the mixed connectivity model [18]. In the serial mode (0-3), the porosities are homogeneously distributed in the polymer matrix. However, in the parallel mode (1-3), the microstructure can be considered as columns of porosity, elongated in the thickness direction. The dielectric constant, as a function of the gas content at low gas volume fractions, shows a good agreement to the predictions of the serial model.

The effect of gaseous volume fraction on the dielectric loss, Tan δ, of the micro-porous PU-PZT composites at 1 kHz, is shown in Fig. 4-d. Tan δ is taken as measure of dielectric loss and is known as loss tangent. In a perfect insulator, there is no consumption of energy, and electric current leads the applied voltage by 90°. However, for commercial dielectrics, this phase angle is less than 90 ° by an angle δ, which is called dielectric loss angle. As shown in Fig. 4-d Tan δ seems to slightly decrease with increasing the gaseous volume fraction which is in agreement with the documented behavior of porous polymers [16, 26].

The dielectric properties of the micro-porous composites, containing PZT powder ranging from 0 vol% to 40 vol% in porous PU matrix, are shown in Fig. 6-a. The dielectric constant of the porous polymer, used as an input for modeling the properties of the micro-porous composites, is experimentally determined as 4.7 for a PU sample containing approximately 60 vol% of gaseous phase. The properties of the random and structured composites are fitted to the models proposed by Yamada [25] and Bowen [27], respectively. The best fit of the experimental data to Yamada's model for the random composites was obtained for $n = 3.6$, which nearly indicates spherical particles. The best fit of the experimental data to Bowens's model, for the structured composites, was obtained for R values of 15. The predictions of the associated models for di-phase composite system consisting of PZT particles and PU polymer are also presented for comparison. Both random and structured di-phase PZT-bulk PU composites show a higher dielectric constant than the micro-porous composites. For the whole PZT range, the improvement in dielectric constant of the micro-porous composites is in accordance with the change in the permittivity of the polymer phase upon addition of the gaseous phase.

The influence of DEP structuring on piezoelectric charge coefficient, d_{33}, of the micro-porous composites is shown in Fig. 6-c. The Young's modulus of the micro-porous PU, as an input for the Van den Ende model, is calculated using the mixed connectivity model, for a perfect 0-3 composite in the serial mode, as shown in Fig. 6-b. The stiffness of a di-phase material in a serial arrangement follows a rule of mixtures. The input stiffness values for the d_{33} simulations was chosen based on the gas content of the composite. The neat PU has a modulus of 4.6 MPa, which decreases significantly with

increasing the gas content and with increasing percentage of open cells.

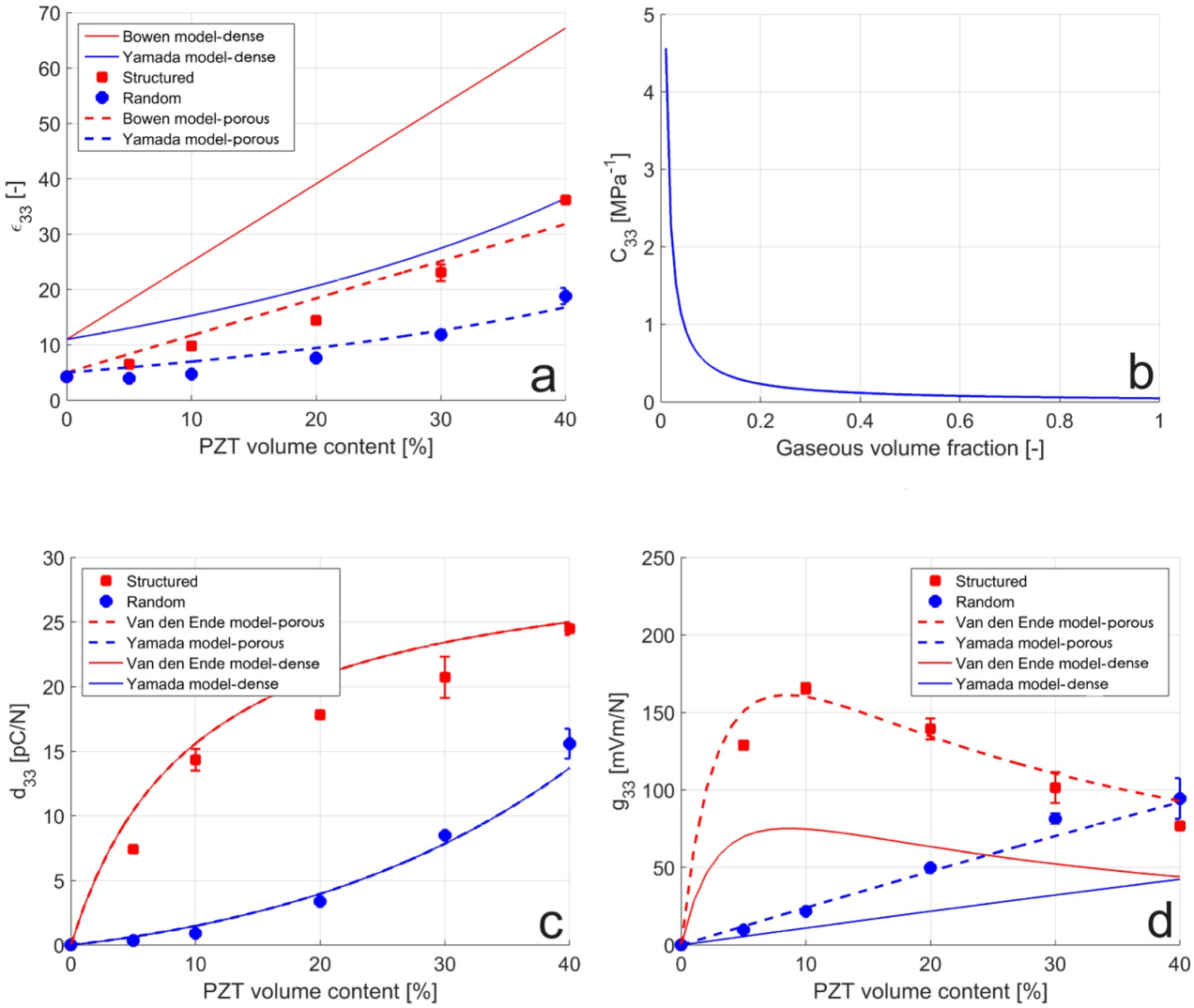

Figure 6: Variation of piezoelectric properties of structured and random composites. (a) Dielectric constant. (b) Variation of stiffness of the micro-porous PU material with the gaseous volume content. (c) d_{33}. (d) g_{33}. Dashed lines indicate the model predictions for PZT-micro-porous PU composites, and the solid lines show properties of PZT-bulk PU composites. Pore volume fraction is 60%.

The measured d_{33} values of structured and random composites are compared with their associated models Yamada [25] and Van den Ende [28]. However, the change in the stiffness of the polymer matrix does not seem to affect the d_{33} value of the PZT-PU composites (see Fig. 6-c), as both bulk and micro-porous composites show a similar behavior. The best fit of the experimental d_{33} data of the random composites to Yamada's model was obtained for $n = 3.6$ and $\alpha = 1$. The high value of α is a clear indication of efficient poling [29, 30]. The best fit of the experimental data to Bowens's model for the structured composites was obtained for R values of 10. The maximum d_{33} value of 25 pC/N is obtained for 40% PZT-micro-porous PU composite, which is twice that of the d_{33} value of 40% PZT-epoxy composite [24]. Moreover, adding the gaseous phase results in a decrease in the stiffness of the polymer matrix, which consequently leads to higher d_{33} values compared to a stiffer polymer matrix [21]. A reduced matrix stiffness assures a minimal absorption of mechanical energy by the matrix upon loading. This results in higher effective strains in the piezoelectric composite material.

The piezoelectric voltage sensitivity, g_{33}, which was calculated by dividing the d_{33} of the composites by its relative

permittivity, is plotted as a function of the PZT volume fraction in Fig. 6-d. The maximum value obtained for the random composites is 94 mV.m/N, at a PZT volume fraction of 40%, while for the structured micro-porous composite, a value of 166 mV.m/N is obtained at a PZT volume fraction of 10%. The predictions of the models for the random and structured bulk systems are also shown. At 10 vol%, the maximum g_{33} of a structured bulk composite is approximately 80 mV.m/N. Therefore, a factor of two improvement in g_{33} is obtained in 10% PZT-micro-porous PU composites by decreasing the dielectric constant of the polymer phase when adding a gaseous content of 60 vol%. The maximum g_{33} reported for structured bulk particulate composites ranges between 70-90 mV.m/N [22, 24]. Addition of the third gaseous phase significantly improves the g_{33} performance of the particulate composites. No degradation in piezoelectric charge constant was observed for 10% structured PZT-micro-porous PU composites, after 1000 cycles at 5% strain. At 30% strain the material fails after 100 cycles.

4 Application

A fully 3D-printed soft hand-shaking robot that feels how hard you squeeze its hand and squeezes back accordingly was created as a metaphor for how soft robotics technology can improve Human-Robot Interaction (HRI). Soft robotic hand used in this work was originally built as a case study for behavior design in 3D-printed soft robotics [31]. The field of soft robotics focuses on the use of materials with YoungâĂŹs moduli in the range of that of soft biological materials in order to improve the safety and adaptability of robots [32]. In the case study of the soft robotic hand, eight air pressure actuators, two air pressure sensors, and structural components were integrated in a single body product using the Additive Manufacturing (AM) process Selective Laser Sintering (SLS). To show the possibility of designing human-like behavior, an interactive setup in which people could shake the robot hand was created as shown in Fig. 7-a.

This robotic hand is actuated through pressurization of flexible air chambers built from the polyurethane TPU92A-1 material. Bending of the thumb and fingers is realized through pressurizing an air chamber with a straight (inextensible) bottom layer and bellow-shaped (extensible) top layer. Two bending actuators that share an inextensible layer were used to create a bidirectional actuator in the wrist. A rotational actuator was created by sweeping a radially expanding bellow over a helical path. The ability to sense a handshake was realized through embedding air chambers in the palm of the hand. Squeezing these air chambers results in an increase in air pressure that can be measured externally from the hand. Touch sensing in the fingers is added by integrating the flexible micro-porous composite sensors (Fig. 7-b) onto the finger tips for tactile feedback [33] as shown in Fig. 7-c. The 10% structured PZT-micro-porous PU composite sensor is sandwiched between two layers of Copper foil, one grounded and one connected to an oscilloscope to record the output signal, and the unit is mounted on the finger tip using insulating tape. To shield the unit from parasitic electromagnetic waves the sensing area is covered using a silver coated plastic shield. The open circuit voltage upon periodic touch with estimated force of 1 N is monitored on an Agilent DSO-X-2002A oscilloscope, as shown in Fig. 7-d, and representative voltage amplitude of 100 mV is measured upon tapping as a function of time. This shows that dielectrophoretically manufactured micro-porous piezoelectric composites have excellent potential for fabrication of large area and flexible touch sensing devices. Furthermore, integration of the piezoelectric and pyroelctric composite sensors that can discriminate between temperature and pressure outputs offers the opportunity of integrating multiple functionalities such as vibrations and

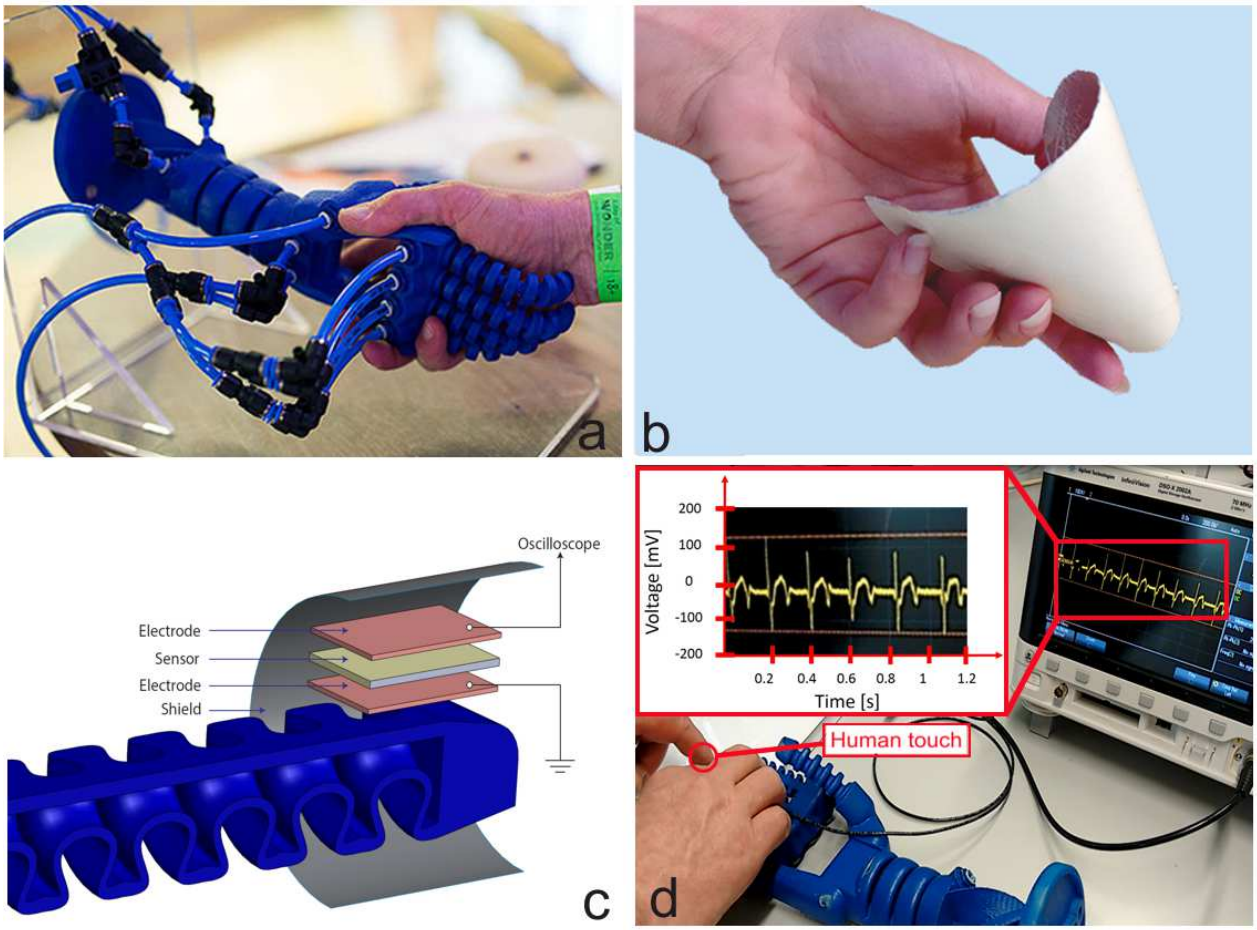

Figure 7: Application of the flexible micro-porous composite sensor in a soft robotic hand. (a) Fully 3D-printed soft robotic hand. (b) Large area flexible micro-porous piezoelectric sensor. (c) Sensor unit lay-up. (d) Recorded signal upon repeatedly touching the sensor.

temperature sensing within one active composite sensor array in future.

5 Conclusions

Creation of uniform spherical micro porosity reduces the dielectric permittivity of PU polymer, which improves the piezoelectric voltage sensitivity of the micro-porous PU-PZT composites significantly. The unique combination of dielectrophoretic structuring of PZT particles in the pore walls and the addition of a gaseous phase to the polymer resin results in the best performance of the particulate composite sensors reported in the literature so far. The g_{33} values of the newly developed micro-porous composites exceed those of the structured di-phase PZT-bulk PU composites (80 mV.m/N), as well as those of the structured PZT-epoxy composites (72-78 mV.m/N) by a factor of two, and more than five times the g_{33} of the bulk PZT ceramics (24-28 mV.m/N). These newly developed piezosensitive composites are demonstrated to be capable of touch sensing in soft robotics applications.

Acknowledgements

This research was carried out under project number M62.3.11438 in the framework of the Research Program of the Materials innovation institute M2i (www.m2i.nl).

References

[1] M. L. Hammock, A. Chortos, B. C.-K. Tee, J. B.-H. Tok, and Z. Bao, "25th anniversary article: The evolution of electronic skin (e-skin): A brief history, design considerations, and recent progress," *Advanced Materials*, vol. 25, no. 42, pp. 5997–6038, 2013.

[2] O. Yilmazoglu, A. Popp, D. Pavlidis, J. J. Schneider, D. Garth, F. Schüttler, and G. Battenberg, "Vertically aligned multiwalled carbon nanotubes for pressure, tactile and vibration sensing," *Nanotechnology*, vol. 23, no. 8, p. 085501, 2012.

[3] M. Ha, S. Lim, J. Park, D.-S. Um, Y. Lee, and H. Ko, "Bioinspired interlocked and hierarchical design of zno nanowire arrays for static and dynamic pressure-sensitive electronic skins," *Advanced Functional Materials*, vol. 25, no. 19, pp. 2841–2849, 2015.

[4] M. Amjadi, K.-U. Kyung, I. Park, and M. Sitti, "Stretchable, skin-mountable, and wearable strain sensors and their potential applications: A review," *Advanced Functional Materials*, vol. 26, no. 11, pp. 1678–1698, 2016.

[5] H. A. K. Toprakci, S. K. Kalanadhabhatla, R. J. Spontak, and T. K. Ghosh, "Polymer nanocomposites containing carbon nanofibers as soft printable sensors exhibiting strain-reversible piezoresistivity," *Advanced Functional Materials*, vol. 23, no. 44, pp. 5536–5542, 2013.

[6] L. Chen, G. Chen, and L. Lu, "Piezoresistive behavior study on finger-sensing silicone rubber/graphite nanosheet nanocomposites," *Advanced Functional Materials*, vol. 17, no. 6, pp. 898–904, 2007.

[7] A. P. Gerratt, H. O. Michaud, and S. P. Lacour, "Elastomeric electronic skin for prosthetic tactile sensation," *Advanced Functional Materials*, vol. 25, no. 15, pp. 2287–2295, 2015.

[8] W. Honda, S. Harada, T. Arie, S. Akita, and K. Takei, "Wearable, human-interactive, health-monitoring, wireless devices fabricated by macroscale printing techniques," *Advanced Functional Materials*, vol. 24, no. 22, pp. 3299–3304, 2014.

[9] J. Dargahi and S. Najarian, "Advances in tactile sensors design/manufacturing and its impact on robotics applications-a review," *Industrial Robot: An International Journal*, vol. 32, no. 3, pp. 268–281, 2005.

[10] J.-S. Heo, J.-H. Chung, and J.-J. Lee, "Tactile sensor arrays using fiber bragg grating sensors," *Sensors and Actuators A: Physical*, vol. 126, no. 2, pp. 312 – 327, 2006.

[11] A. Kulkarni, H. Kim, J. Choi, and T. Kim, "A novel approach to use of elastomer for monitoring of pressure using plastic optical fiber," *Review of Scientific Instruments*, vol. 81, no. 4, 2010.

[12] M. Zirkl, A. Sawatdee, U. Helbig, M. Krause, G. Scheipl, E. Kraker, P. A. Ersman, D. Nilsson, D. Platt, P. BodÃű, S. Bauer, G. Domann, and B. Stadlober, "An all-printed ferroelectric active matrix sensor network based on only five functional materials forming a touchless control interface," *Advanced Materials*, vol. 23, no. 18, pp. 2069–2074, 2011.

[13] I. Graz, M. Krause, S. Bauer-Gogonea, S. Bauer, S. P. Lacour, B. Ploss, M. Zirkl, B. Stadlober, and S. Wagner, "Flexible active-matrix cells with selectively poled bifunctional polymer-ceramic nanocomposite for pressure and temperature sensing skin," *Journal of Applied Physics*, vol. 106, no. 3, 2009.

[14] J.-H. Lee, H.-J. Yoon, T. Y. Kim, M. K. Gupta, J. H. Lee, W. Seung, H. Ryu, and S.-W. Kim, "Micropatterned p(vdf-trfe) film-based piezoelectric nanogenerators for highly sensitive self-powered pressure sensors," *Advanced Functional Materials*, vol. 25, no. 21, pp. 3203–3209, 2015.

[15] W. Wu, X. Wen, and Z. L. Wang, "Taxel-addressable matrix of vertical-nanowire piezotronic transistors for active and adaptive tactile imaging," *Science*, vol. 340, no. 6135, pp. 952–957, 2013.

[16] B. Krause, G.-H. Koops, N. F. van der Vegt, M. Wessling, M. Wubbenhorst, and J. van Turnhout, "Ultralow-k dielectrics made by supercritical foaming of thin polymer films," *Advanced Materials*, vol. 14, no. 15, pp. 1041–1046, 2002.

[17] D. Kwon, T.-I. Lee, J. Shim, S. Ryu, M. S. Kim, S. Kim, T.-S. Kim, and I. Park, "Highly sensitive, flexible, and wearable pressure sensor based on a giant piezocapacitive effect of three-dimensional microporous elastomeric dielectric layer," *ACS Applied Materials & Interfaces*, vol. 8, no. 26, pp. 16922–16931, 2016.

[18] C. Dias, *Ferroelectric composites for pyro- and piezoelectric applications*. PhD thesis, School of electronic engineering and computer systems, University of Wales, Bangor, UK, 1994.

[19] N. Chand and J. Sharma, "Influence of porosity on resistivity of polypropylene foams," *Journal of Cellular Plastics*, vol. 48, no. 1, pp. 43–52, 2012.

[20] K. C. Khemani, *Polymeric Foams*. Washington, DC: American Chemical Society, 1997.

[21] S. van Kempen, " Optimisation of Piezoelectric Composite Materials Design through Improved Materials Selection and Property Prediction Methods," Master's thesis, Faculty of Aerospace Engineering, Delft University of Technology, Delft, The Netherlands, 2012.

[22] H. Khanbareh, S. van der Zwaag, and W. Groen, "Effect of dielectrophoretic structuring on piezoelectric and pyroelectric properties of PT-epoxy composites," *Smart Materials and Structures*, vol. 23, no. 10, p. 105030, 2014.

[23] M. Gutiérrez, H. Khanbareh, and S. van der Zwaag, "Computational modeling of structure formation during dielectrophoresis in particulate composites," *Computational Materials Science*, vol. 112, Part A, pp. 139 – 146, 2016.

[24] D. A. van den Ende, *Structured piezoelectric composites, materials and applications*. PhD thesis, Faculty of Aerospace Engineering, Delft University of Technology, The Netherlands, 2012.

[25] T. Yamada, T. Ueda, and T. Kitayama, "Piezoelectricity of a high-content lead zirconate titanate polymer composite," *Journal of Applied Physics*, vol. 53, p. 4328, 1982.

[26] A. B. Martin Straat, Igor Chmutin, "Dielectric properties of polyethylene foams at medium and high frequencies," *Annual Transactions of the Rheology Society*, vol. 18, pp. 1–10, 2010.

[27] C. P. Bowen, R. E. Newnham, and C. A. Randall, "Dielectric properties of dielectrophoretically assembled particulate-polymer composites," *Journal of Materials Research*, vol. 13, pp. 205–210, 1998.

[28] D. van den Ende, B. Bory, W. Groen, and S. van der Zwaag, "Improving the d33 and g33 properties of 0-3 piezoelectric composites by dielectrophoresis," *Journal of Applied Physics*, vol. 107, no. 2, 2010.

[29] H. Khanbareh, S. van der Zwaag, and W. Groen, "Piezoelectric and pyroelectric properties of conductive polyethylene oxide-lead titanate composites," *Smart Materials and Structures*, vol. 24, no. 4, p. 5020, 2015.

[30] H. Khanbareh, S. van der Zwaag, and W. Groen, "In-situ poling and structurization of piezoelectric particulate composites," *Journal of Intelligent Material Systems and Structures*, 2017.

[31] R. B. Scharff, E. L. Doubrovski, W. A. Poelman, P. P. Jonker, C. C. Wang, and J. M. Geraedts, "Towards behavior design of a 3d-printed soft robotic hand.," in *Soft Robotics: Trends, Applications and Challenges*, Springer, 2016.

[32] D. Rus and M. T. Tolley, "Design, fabrication and control of soft robots.," *Nature*, vol. 521, pp. 467–475, 2015.

[33] M. I. Tiwana, S. J. Redmond, and N. H. Lovell, "A review of tactile sensing technologies with applications in biomedical engineering," *Sensors and Actuators A: Physical*, vol. 179, pp. 17 – 31, 2012.